

UNOBTRUSIVE BALLISTOCARDIOGRAPHY USING AN  
ELECTROMECHANICAL FILM TO OBTAIN PHYSIOLOGICAL  
SIGNALS FROM CHILDREN WITH AUTISM SPECTRUM DISORDER

by

STEVE RUBENTHALER

B.S., Kansas State University, 2011

A REPORT

submitted in partial fulfillment of the requirements for the degree


MASTER OF SCIENCE

Department of Electrical and Computer Engineering  
College of Engineering

KANSAS STATE UNIVERSITY  
Manhattan, Kansas

2014

Approved by

  
Major Professor  
Steve Warren

# **Copyright**

STEVE RUBENTHALER

2014

## Abstract

Polysomnography is a method to obtain physiological signals from individuals with potential sleep disorders. Such physiological data, when acquired from children with autism spectrum disorders, could allow caregivers and child psychologists to identify sleep disorders and other indicators of nighttime well-being that affect their quality of life and ability to learn. Unfortunately, traditional polysomnography is not well suited for children with autism spectrum disorder because they commonly have an aversion to unfamiliar objects – in this case, the numerous wires and electrodes required to perform a full polysomnograph. Therefore, an innovative, unobtrusive method for gathering relevant physiological data must be designed.

This report discusses several methods for obtaining a ballistocardiogram (BCG), which is a representation of the ballistic forces created by the heart during the cardiac cycle. A ballistocardiograph design is implemented using an electromechanical film placed under the center of a bed sheet. While an individual sleeps on the bed, the circuitry attached to the film extract and amplify the BCG data, which are then streamed to a computer through a LabVIEW interface and stored in a text file. These data are analyzed with a MATLAB algorithm which uses autocorrelation and linear predictive coding in the time domain to sharpen the signal. Frequency-domain peaks are then extracted to determine average heart rate every ten seconds.

Initial tests involved four participants (student members of the research team) who laid in four positions: on their back, stomach, right side, and left side, yielding 16 unique data sets. Each participant laid in at least one position that allowed for accurate tracking of heart rate, with seven of the 16 signals demonstrating heart rates with less than 2% error when compared to heart rates acquired with a commercial pulse oximeter. The stomach position appeared to offer the lowest total error, while lying on the right side offered the highest total error. Overall, heart rates acquired from this initial set of participants exhibited an average error of approximately 2.5% for all four positions.

# Table of Contents

List of Figures .....	v
List of Tables .....	vi
Chapter 1 - Introduction.....	1
1.1 Research Contribution and Significance.....	1
1.2 Health Parameter Monitoring in People with Disabilities .....	2
1.3 Report Outline.....	2
Chapter 2 - Background and Prior Research.....	3
2.1 Load Cells .....	3
2.2 Electromechanical Film .....	3
2.3 Hydraulic Sensors .....	4
2.4 Fiber Optic Sensors.....	4
Chapter 3 - Methods.....	6
3.1 General Approach .....	6
3.2 System Integration .....	6
3.3 BCG Circuit .....	7
3.3.1 Preamplifier.....	8
3.3.2 Gain Stage .....	10
3.4 Software .....	10
3.4.1 Raw Data.....	10
3.4.2 High Pass Filter .....	11
3.4.3 Making Heart Rate More Distinct.....	12
3.4.4 Heart Rate Estimation .....	16
3.5 Process for Participants.....	19
Chapter 4 - Results.....	20
4.1 Measurements .....	20
4.2 Subject Results.....	25
Chapter 5 - Future Work and Conclusions .....	28
References.....	29
Appendix A - MATLAB Script .....	31

## List of Figures

Figure 1. Block diagram. ....	7
Figure 2. Circuit schematic and prototype. ....	8
Figure 3. Representative raw BCG data. ....	11
Figure 4. Representative BCG data at the output of the highpass filter. ....	12
Figure 5. Representative BCG spectrum obtained with an FFT. ....	13
Figure 6. Autocorrelated BCG data. ....	14
Figure 7. Spectrum of the autocorrelated data in the previous figure. ....	14
Figure 8. Magnitude spectrum obtained using linear predictive coding. ....	15
Figure 9. Magnitude spectrum obtained using both autocorrelation and LPC. ....	16
Figure 10. Ideal magnitude spectrum for determining heart rate. ....	17
Figure 11. Non-ideal magnitude spectrum for determining heart rate. ....	18
Figure 12. Heart rate data from Subject 1 lying on their back. ....	21
Figure 13. Heart rate data from Subject 1 lying on their stomach. ....	21
Figure 14. Heart rate data from Subject 1 lying on their right side. ....	21
Figure 15. Heart rate data from Subject 1 lying on their left side. ....	21
Figure 16. Heart rate data from Subject 2 lying on their back. ....	22
Figure 17. Heart rate data from Subject 2 lying on their stomach. ....	22
Figure 18. Heart rate data from Subject 2 lying on their right side. ....	22
Figure 19. Heart rate data from Subject 2 lying on their left side. ....	22
Figure 20. Heart rate data from Subject 3 lying on their back. ....	23
Figure 21. Heart rate data from Subject 3 lying on their stomach. ....	23
Figure 22. Heart rate data from Subject 3 lying on their right side. ....	23
Figure 23. Heart rate data from Subject 3 lying on their left side. ....	23
Figure 24. Heart rate data from Subject 4 lying on their back. ....	24
Figure 25. Heart rate data from Subject 4 lying on their stomach. ....	24
Figure 26. Heart rate data from Subject 4 lying on their right side. ....	24
Figure 27. Heart rate data from Subject 4 lying on their left side. ....	24

## List of Tables

Table 1. Error and standard deviation for all data sets. ....	25
Table 2. Heart rate error for each position. ....	26
Table 3. Heart rate error for each subject. ....	27

# Chapter 1 - Introduction

A person may need to have their physiological data continuously monitored during the night for a variety of reasons, including sleep disorder diagnosis. Current nighttime monitoring technologies, such as those incorporated in a traditional polysomnograph [1], require wires and straps to be attached to a subject. However, these tools can be inconvenient for subjects during sleep, and this inconvenience can be even greater for children with severe disabilities because they commonly have an aversion to unfamiliar objects. Heart rate monitoring, in particular, is seen as a challenge by those that work with such subjects because these children will most certainly pull off the wires and finger clips, thereby complicating the process of obtaining accurate data. If an unobtrusive method to measure, e.g. a disabled child's heart rate, could be utilized, then caregivers could acquire these data without disrupting the child's sleep. The purpose of this research is to design and evaluate an unobtrusive method to gather such physiological data from a sleeping child.

## 1.1 Research Contribution and Significance

Because almost 1.1% of children today have autism spectrum disorder (ASD) coupled with a disorder [2], research is needed to create effective, unobtrusive health parameter monitors that can be used during the night. Destructive behavior is a serious concern for children with ASD, as it often includes hitting themselves or others. Children with ASD can also exhibit tantrums that increase behavior volatility [3]. A primary goal of paraeducators and child psychologists that work with these children is to teach them life skills such as such as personal hygiene and feeding themselves, but children with ASD must also be taught how to engage self-control and stop their destructive behavior. The challenge of teaching these children increases when they have sleep disorders because, similar to neurotypical children without ASD, a non-restful night's sleep can hinder their ability to learn. Currently, paraeducators who specialize in teaching and caring for children with ASD do not have access to effective resources or feedback regarding the quality or quantity of their student's sleep for a given night. If a paraeducator knew a child had experienced a disruption during the previous night's sleep, the paraeducator could adjust the educational workload or rate.

## **1.2 Health Parameter Monitoring in People with Disabilities**

One out of sixty eight children under eight years old has ASD [4], and up to 80% of children with ASD also suffer from sleep disorders [2]. A polysomnograph (PSG), a traditional tool to diagnose various sleep disorders, typically monitors several health parameters, including brain activity, eye movement, muscle activity, heart rhythm, respiratory rate, and blood oxygen saturation [1]. PSG sensors are attached to the subject while they sleep, and the resulting data are analyzed to make sleep diagnoses. Even with an approach designed to minimize the amount of wires and straps, a subject can be attached to more than ten wires and straps while sleeping [1], thereby causing discomfort for even neurotypical subjects without documented disabilities. Subjects can take multiple nights to become accustomed to the wires to obtain accurate results.

PSGs are envisioned to be extraordinarily challenging to conduct on people with ASD because of their obtrusiveness. Individuals with ASD, especially children, are sensitive to their surroundings, often tearing off monitoring wires or experiencing fright to such an extreme that accurate data are impossible to obtain. This makes a typical PSG impractical with this population. Therefore, a new method for determining nighttime health parameters is needed.

## **1.3 Report Outline**

Chapter 2 contains background information that gives context to the research and contributions in this report. The chapter describes current monitoring systems for gathering heart rate and compares and contrasts several unobtrusive methods to obtain heart rate. Chapter 3 applies a system level look at the unobtrusive approach utilized here and then describes the circuitry and software algorithms used to acquire and process a ballistocardiogram (BCG). The chapter concludes with the process used to gather data from subjects that were part of the research and development team. Chapter 4 depicts sixteen graphs (four individuals, each lying in four positions) of heart rate versus time for the proposed method versus a commercial pulse oximeter. Chapter 4 then presents the related error percentages and standard deviations. Finally, Chapter 5 offers insights based on these research findings and offers possibilities for future work.



## **Chapter 2 - Background and Prior Research**

This chapter includes background information that gives context to the contributions of this report. The following sections compare methods to obtain a time-domain ballistocardiogram (BCG), which represents the ballistic forces created by the heart during the cardiac cycle. This signal contains information regarding multiple cardiopulmonary parameters, including heart rate and respiration rate. Four methods are included here, and the advantages and disadvantages of each approach are noted given the goal of obtaining heart rate from children with ASD. Degree of unobtrusiveness, subject safety, and design practicality are of particular interest.

### **2.1 Load Cells**

Much research has focused on BCGs acquired with load cells, making them an appealing place to start for this type of work [5, 6]. Load cells are sensors that transduce pressure into voltage through resistive, capacitive, or inductive means. Typical setups consist of potentially four load cells placed under the frame of a chair or bed, one on each corner. Load cells for this BCG method slightly elevate the bed and must be hidden. A possibility exists for the bed to slip off of the load cells.

In addition to detecting body movements, if the subject lies still, then load cells can detect small changes in pressure due to heart activity and lung expansion/relaxation, where the resulting BCGs offer sufficient sensitivity to monitor heart rate and respiration rate. However, BCGs based on load cells can be expensive because four cells and four circuits are required, where the circuit amplification must self-adjust depending on subject movement. Load cells require a power source and have a constant DC voltage because the bed and the subject exert constant pressure [5].

### **2.2 Electromechanical Film**

Electromechanical film is a flat flexible sheet consisting of a sensing element constructed of elastic electrets Emfit film and three layers of polyester film that sandwich two flat aluminum electrodes [7]. This film converts pressure into charge through the structure of layers of this film, creating a voltage across the electrodes that can be amplified to achieve a usable voltage. No dc offset needs to be applied in the circuit because the electromechanical film creates charge based upon the change in pressure. Once this usable voltage is available, electromechanical film acts

similarly to piezoelectric film, meaning that circuitry designed for use with piezoelectric film can be adapted for use with electromechanical film. In the context of the work presented here, the electromechanical film can lie in the middle of the bed, in the approximate location of the subject's heart, and detect small pressure changes related to cardiac and lung activity, meaning that signal quality is related to the person's position on the bed. Because of the film's sensing method, it can be placed under the bed sheets, making the film reasonably undetectable to the subject. Of the techniques noted in this report, the electromechanical film is the only method that does not require external power to the sensor – it is a 'passive' sensor. Electromechanical film is also appealing from the viewpoint of subject safety, since no electrode contact to the subject is required. In addition, only one film and one circuit are needed, so the electromechanical film approach is less expensive than the load cell and hydraulic methods for obtaining a BCG [8].

### **2.3 Hydraulic Sensors**

A hydraulic BCG sensor can be comprised of a three inch wide, twenty inch long discharged hose filled 70% with water, with an integrated pressure sensor to measure vibrations passing through the liquid in the bag [9]. The sensitivity of these bags allows them to be placed under the subject's mattress – they are hidden. These relatively inexpensive sensors can gather a signal throughout the entire bed width, and several of the fluid-filled bags can be placed next to each other. Four bags were used during pulse rate estimation with a hydraulic bed sensor by Su, Ho et al., making this method more costly than the fiber optic and electromechanical film BCGs because of the use of four sensors and increased circuitry. Circuit construction for this hydraulic BCG sensor is more straightforward than the electromechanical film because the pressure sensor in each discharged hose yields a voltage, but the circuit has added complications because the sensor needs power and several sensors are required to acquire a signal over the entire bed [9].

### **2.4 Fiber Optic Sensors**

A fiber optic BCG sensor uses a fiber optic cable woven into a pillow and connected to a light source [10]. A light detector at the end of the fiber optic cable acquires the BCG signal. A fiber optic cable can be completely hidden in a pillow so that the subject is unaware of its presence, but this approach requires that wires protrude out the back of the pillow, which causes a safety hazard if the subject moves the pillow. It is reasonable to assume that these fiber optic cables could be woven into a mattress instead of a pillow for use on children with ASD to avoid

this safety hazard. According to previous research, the sensor is sensitive enough to gather all necessary BCG signal components, but the sensor is not a commercial product, which implies that the sensitivity will fluctuate depending on how the fiber optic cable is woven through the pillow when it is constructed in the laboratory. The inexpensive nature of the sensor parts infers that the fiber optic BCG sensor can be inexpensive compared to other investigated methods, although this BCG sensor requires a light source to be focused into the fiber optic cable, increasing circuit complexity. In addition, the fiber optic BCG sensor is a new use of the technology, and information is limited regarding the affiliated BCG circuitry [10].

## Chapter 3 - Methods

This chapter describes the approach used to realize an unobtrusive solution for acquiring a sleeping person's heart rate. The solution includes a circuit to obtain raw electrical signals from an electromechanical film, where these signals are streamed into a computer for further filtering and extraction of heart rate.

### 3.1 General Approach

After examining the potential methods for unobtrusive heart rate monitoring as summarized in Chapter 2, the electromechanical film approach was chosen given its benefits and potential to provide high-quality BCG data. This type of film transduces pressure into charge, which can then be converted to an electrical voltage and digitized for further analysis. For these efforts, an electromechanical film was inserted under bed sheets in the approximate location of a sleeping person's heart, allowing the pressure waveform induced by cardiac and lung activity to be received by the electromechanical film and converted into a charge [8]. Circuit and algorithm details are noted in the following sections.

### 3.2 System Integration

The BCG system was set up as depicted in Figure 1. The electromechanical film's output, or raw signal, was input to a circuit which converted the charge into usable voltage. The circuit was powered by a Sorensen XPH-35-4T power supply. The analog circuit output was then sent to a National Instruments myDAQ personal data acquisition unit, where it was converted to a digital signal ( $f_s = 150$  Hz, 16 bits) and sent to a LabVIEW 2012 virtual instrument that displayed the data and then saved them to disk.

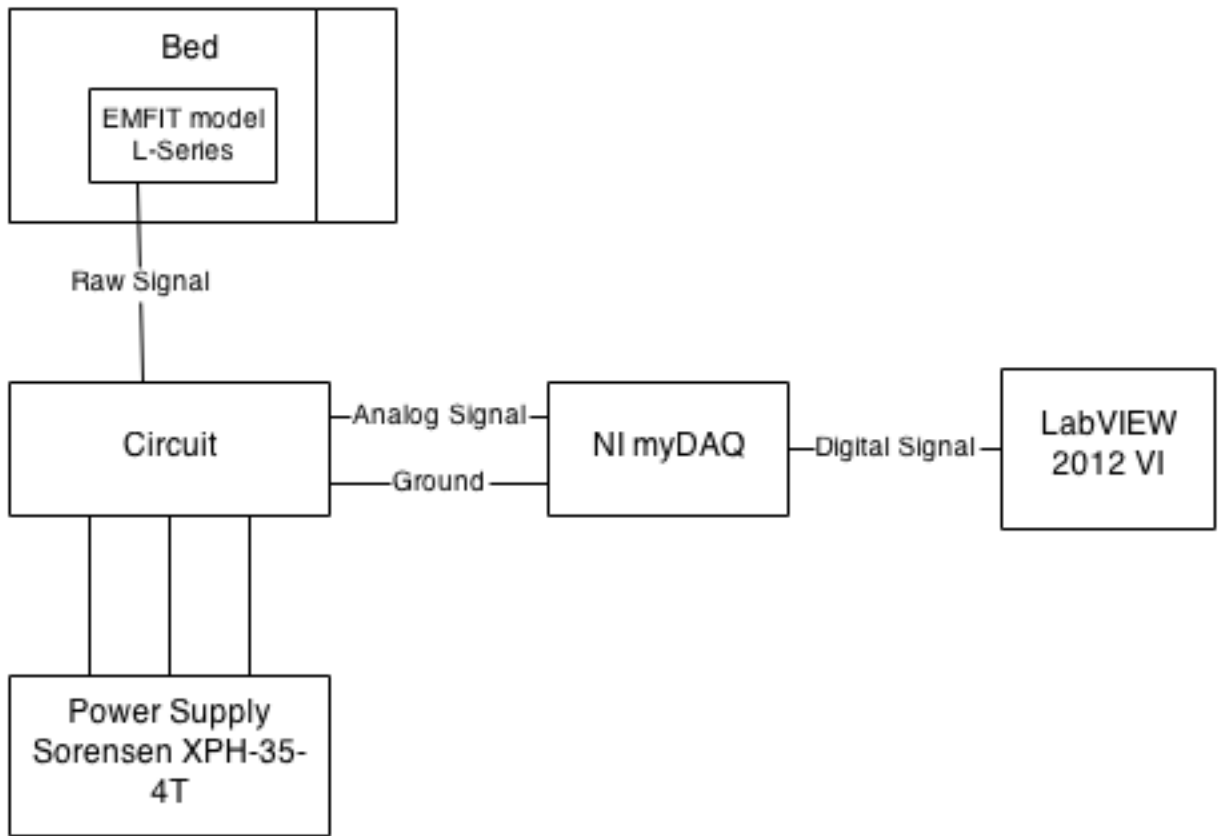


**Figure 1. Block diagram.**

### 3.3 BCG Circuit

The first stage of the circuit had to be able to convert charge from the electromechanical film (EMFIT model L-Series, 290 mm x 300 mm) into a usable voltage that could be sent to the data acquisition unit. For this BCG circuit, film-manufacturer suggestions were used to maintain a consistent standard of circuit design. However, the manufacturer neglected to suggest a method to connect the electromechanical film to the circuit board. Therefore, a ribbon cable with one end soldered to the film and the other end attached to a female 10-pin connector was used. The corresponding male connector was soldered onto the circuit board for ease of attachment to the circuit and the ability to store or change the electromechanical film.

Figure 2 illustrates the final schematic for the circuit along with the circuit board prototype. A 300 mil surface-mount solder board was used to construct the prototype. Because of the 300 mil spacing on this proto-board, 8-pin DIP (300 mil) and through-hole-to-surface-mount sockets were used. All capacitors and resistors were 0805 (2012 metric) to fit the pads of

the surface mount solder board. Both 0.1  $\mu\text{F}$  ceramic capacitors and 4.7  $\mu\text{F}$  tantalum capacitors were used on each integrated circuit chip for bypass capacitors. The following paragraphs explain the circuit design parameters in more detail.

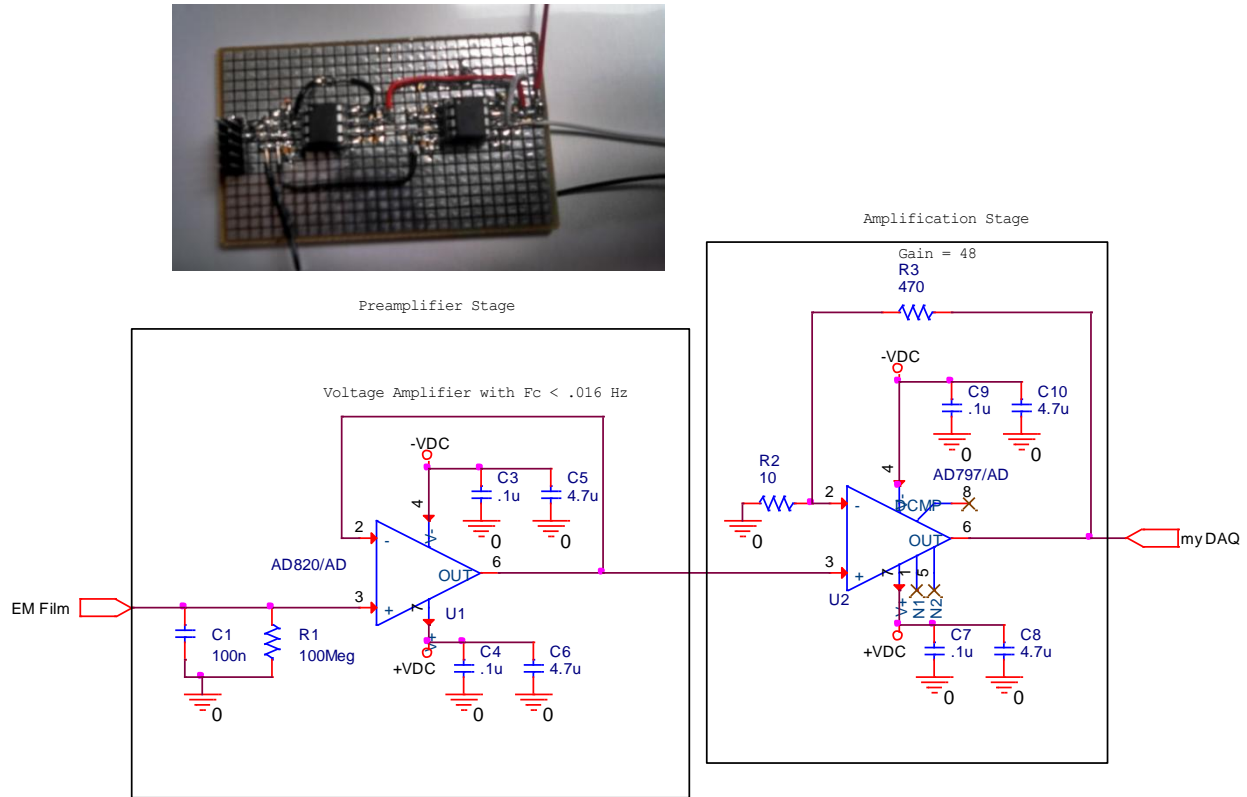


**Figure 2. Circuit schematic and prototype.**

### 3.3.1 Preamplifier

First, the BCG circuit required a preamplifier that could convert charge stored on the film electrodes into a sensible voltage. In addition to use of the AD 820 operational amplifier, EMFIT, the electromechanical film manufacturer, suggested two basic operational amplifiers. The first amplifier, which is a charge amplifier that accurately converts a charge into voltage, is preferred because the capacitance (size) of the electromechanical film is not factored into the time constant or voltage signal amplitude, as described in Equations 1 and 2, respectively [11]:

$$\text{Time Constant} = R * C, \quad (1)$$

where  $R$  ( $\Omega$ ) is the resistance,  $R1$ , and  $C$  (F) is the capacitance  $C1$ . This lowpass circuit passes frequencies that are lower than the following criterion:

$$F_c = \frac{1}{2 * \pi * R * C}. \quad (2)$$

The amplitude of the voltage signal,  $V_p$  (V) out of the first stage in Figure 2 is

$$V_p = \frac{1}{C} * S_q * F_p, \quad (3)$$

where  $C$  (pF) is the capacitance,  $S_q = (25 \text{ (pC/N)})$  is the sensitivity, and  $F_p$  (N) is amplitude of the force.

EMFIT also suggested a voltage amplifier for the preamplifier circuit. This operational amplifier also successfully converts charge to a usable voltage, but the film's capacitance must be added into  $C$  used in Equations 1 and 2. Additional capacitance in the equations results in a higher  $RC$  time constant, lower corner frequency from Equation 2, and lower signal voltage amplitude [11].

The majority of usable signal information for a BCG resides in the frequency range of approximately 0.7 to 10 Hz. To maintain information associated with respiration rate, frequencies must be saved down to 0.1 Hz [12]. The signal originating from the electromechanical film is positive for applied pressure and negative for released pressure. Therefore, both amplifier designs contain non-electrolytic capacitors to maintain consistency on the positive and negative signals. Manufacturer suggestions for capacitors were 100 nF and a resistor of 100 M $\Omega$  [11]. When incorporating  $C = 100 \text{ nF}$  and  $R = 100 \text{ M}\Omega$ , the corner frequency is

$$f_c = \frac{1}{2 \Omega * 100 \text{ M}\Omega * 100 \text{ nF}} \approx 16 \text{ mHz} \quad (4)$$

Equation 4 indicates that the charge amplifier would not maintain full heart rate data amplitudes. However, the voltage amplifier (as illustrated in the left half of Figure 2) helps. The film capacitance is described by the manufacturer as in Equation 5 [7].

$$C_{film} = 22 \frac{\text{pF}}{\text{cm}^2} * Area \text{ (cm}^2\text{)} \quad (5)$$

The electromechanical film is 290 mm x 300 mm, so  $C_{film}$  would be

$$C_{film} = 22 \frac{\text{pF}}{\text{cm}^2} * 8700(\text{cm}^2) = 191.4 \text{ nF} \quad (6)$$

Use of this additional capacitance yields a corner frequency for the voltage amplifier of

$$f_c = \frac{1}{2 * \Omega * 100 \text{ M}\Omega * (100 \text{ nF} + 191.4 \text{ nF})} \approx 5.5 \text{ mHz} \quad (7)$$

Equation 7 also indicates that the voltage amplifier would not provide a corner frequency up to 10 Hz to maintain full heart rate data magnitude. This problem is dealt with in the next section by increasing the gain stage.

### 3.3.2 Gain Stage

A gain stage was required as the next portion of the circuit, as noted in the right half of Figure 2. Because the heart rate component in a BCG can be in the  $\mu\text{V}$  range, a gain over 25 was required [13]. To obtain a higher quality signal, a low-noise op amp was used to keep the signal-to-noise ratio high. Therefore, an ultra-low noise amp (AD797) was used, and data sheet recommendations were followed to minimize noise. For gains greater than 35, the AD797 data sheet suggested using an  $R_2$  of  $10\ \Omega$  and an  $R_3$  equal to Equation 8 [14]:

$$R_3 = (\text{Gain} - 1) * 10 \quad (8)$$

After studying several gains, 50 was used for the final gain. Because of resistor supply limitations, the following resistors were used:  $R_2 = 10\ \Omega$  and  $R_3 = 470\ \Omega$ .

## 3.4 Software

The primary software features required for this study were upgradeability of the user interface and flexibility with regard to algorithmic computations. Therefore, LabVIEW 2012 was chosen because it is compatible with the NI myDAQ data acquisition unit ( $f_s = 150\ \text{Hz}$ , 16 bits), simplifying data acquisition after the signal was converted to a digital stream. LabVIEW also offers flexibility with regard to the visual appearance of the virtual instruments. LabVIEW's MathScript RT Module was employed so that MATLAB scripts could be used and modified as processing needs changed. A final MATLAB script, as presented in Appendix A, was used to test versions of the processing algorithms using previously recorded data sets and to observe these results in a graphical format.

### 3.4.1 Raw Data

The LabVIEW program for this study began as a stock LabVIEW program. Once raw data were input into the MathScript block, several variables were added so the MathScript code could be dynamic for any input. These raw data were studied to determine what filtering to do first. Figure 3 illustrates a typical raw data set for an adult test subject, where the subject is lying on their stomach above the electromechanical film.



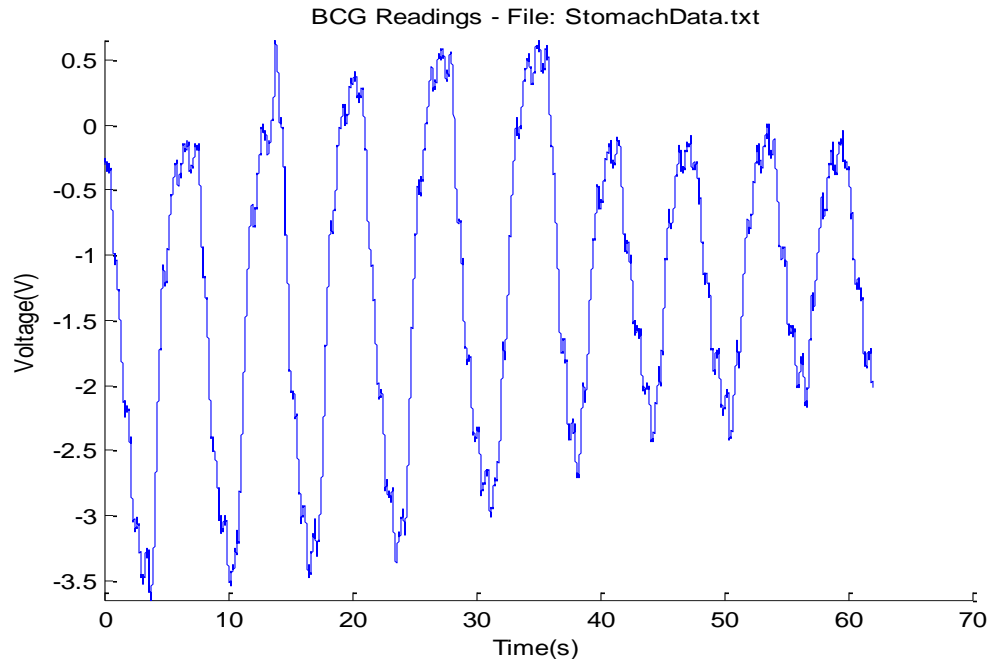


**Figure 3. Representative raw BCG data.**

Figure 3 primarily exhibits respiration data because pressure resulting from chest movement is greater than pressure from heart activity. The data in Figure 3 indicate that time between respiration cycles was approximately 7 seconds, offering a respiration rate of approximately 0.11 breaths per second, which is in the respiration range of an average adult: 5 to 20 breaths per minute or 0.08 Hz to 0.33 Hz.

### ***3.4.2 High Pass Filter***

To obtain heart rate from a typical data set, a BCG's respiration component must first be filtered out while maintaining the heart rate component. Further, to retain use of this circuit for both children and adults, the fact that children have higher respiration rates than adults, even as high as 30 breaths per minute at 3 years of age, must be taken into account. Therefore, 30 breaths per minute (0.5 Hz) was used as the frequency where the high pass digital filter started to transition from a gain of zero to a gain of one. Children also have a higher heart rate than adults, from 80 to 120 bpm at 3 years old, so the minimum heart rate for adults, 60 bpm (1 Hz), was used as the frequency where the high pass digital filter finished its transition from a gain of zero to a gain of one. A finite impulse response software filter implemented in MathScript was chosen for the high pass filter design. Because this software filter specifically filters the signal and the use of a static filter order changes filter efficiency depending on sample frequency, a dynamic

filter order was used so that efficiency remained constant no matter how fast a sample frequency was used. The filter order provided for this high pass filter was

$$\text{Filter Order} = 2 * \text{round}\left(\frac{SR}{2f_c}\right), \quad (9)$$

where  $SR$  is the LabVIEW sample rate and  $f_c$  is the corner frequency chosen. After selecting the filter order, the first-round implementation of the MATLAB script (Appendix A) was used to view the results. Figure 4 illustrates one data set after application of the high pass filter. The filtered data set predominantly contains heart rate components, with minimal respiration data as a varying baseline.

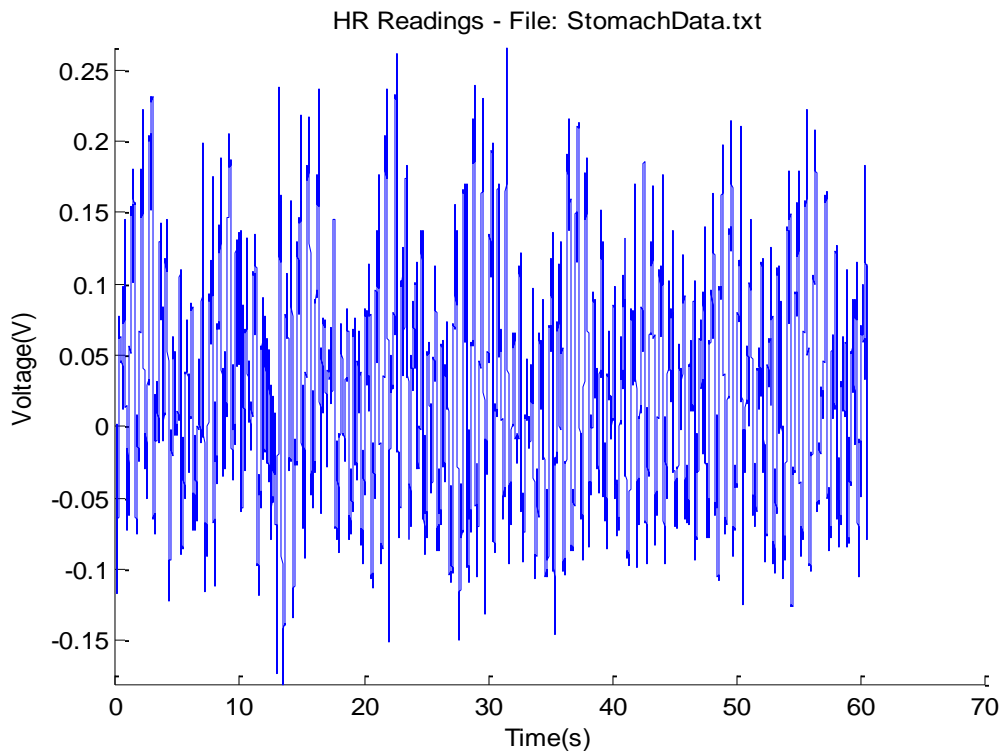


**Figure 4. Representative BCG data at the output of the highpass filter.**

### ***3.4.3 Making Heart Rate More Distinct***

In addition to a highpass filter, a fast Fourier transform (FFT) was added to the MATLAB script to determine the most prevalent frequencies in a BCG (see Figure 5). The resulting FFTs should then exhibit peaks where heart rate is distinct, and a range of frequencies could also be determined for heart rate for a given data set. The downside with using this FFT approach alone is that FFT resolution is solely determined by the acquisition time (the time-

domain length) of the data set, possibly zero padded to the next highest time that incorporates  $2^n$  data points. In order to obtain, e.g., a spectral resolution which indicates the difference between 65 bpm and 66 bpm, the data set must be 60 seconds long.

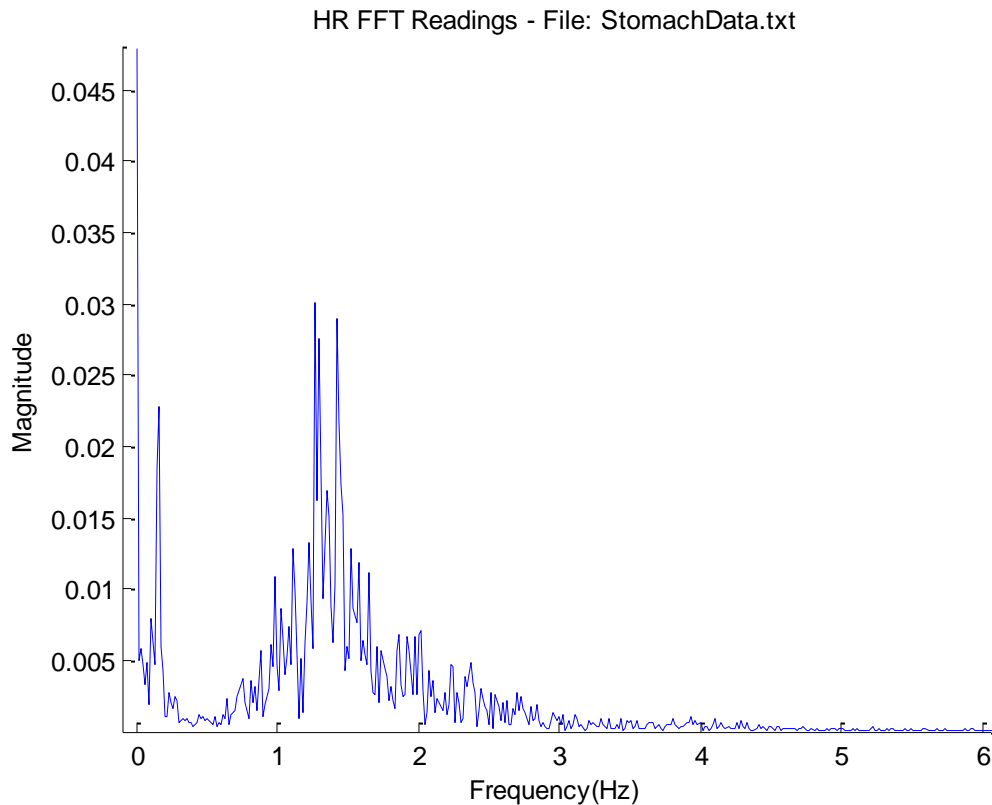


**Figure 5. Representative BCG spectrum obtained with an FFT.**

To address this issue, the algorithm adds a technique in the time domain to make the signal more distinct and then returns to the frequency domain for heart rate determination. Two methods of time-domain manipulation were tested to determine which method offered more distinct results. First, autocorrelation, or cross-correlating the signal with itself, was used. This technique, often used to find repeating patterns, can be used to increase the distinctiveness of the repeating heartbeat. When autocorrelation was added to the MATLAB script, the first 25% and last 25% of the signal were discarded in order to obtain a stronger indication of the repeated portion of the signal. Then, the magnitude spectrum of the autocorrelation result was analyzed to determine what kind of improvement had been achieved. Figure 6 displays the autocorrelation of a representative signal, and Figure 7 displays the magnitude spectrum of that autocorrelated signal

[15]. The spectrum in Figure 7 shows more distinct peaks relative to the spectrum in Figure 5 and contains less noise.

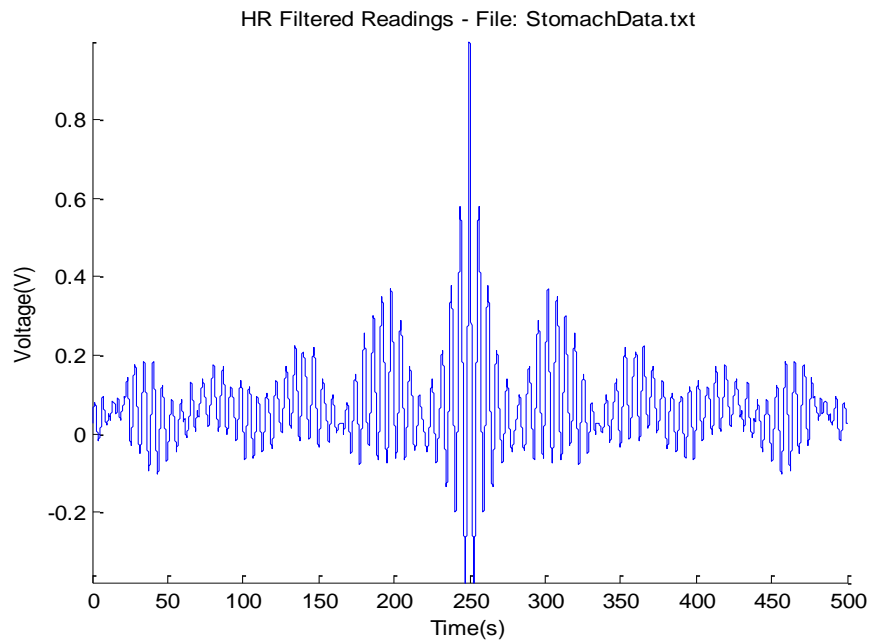


**Figure 6. Autocorrelated BCG data.**

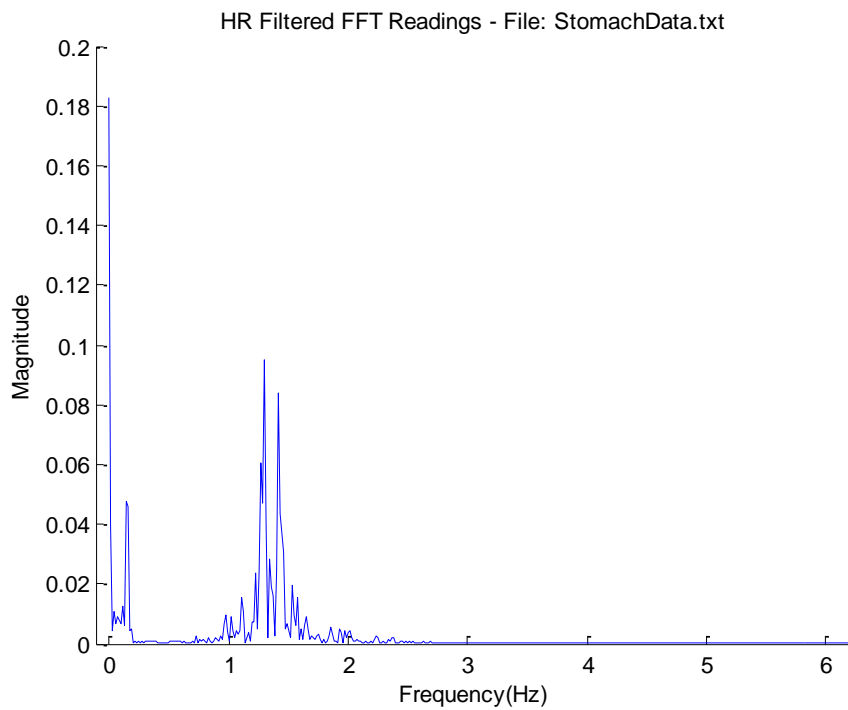


**Figure 7. Spectrum of the autocorrelated data in the previous figure.**

The next method, linear predictive coding (LPC), determines coefficients of a  $p^{\text{th}}$ -order polynomial to predict the current value of a time series based on previous data by minimizing the least squares error between the polynomial and the data set. The magnitude response of the  $p^{\text{th}}$ -order polynomial is then calculated with an FFT. Figure 8 illustrates the magnitude spectrum of a 256<sup>th</sup>-order polynomial after LPC was applied. Smoothing effects in Figure 8 are due to the algorithm that the LPC method used to minimize the least squares error [16].

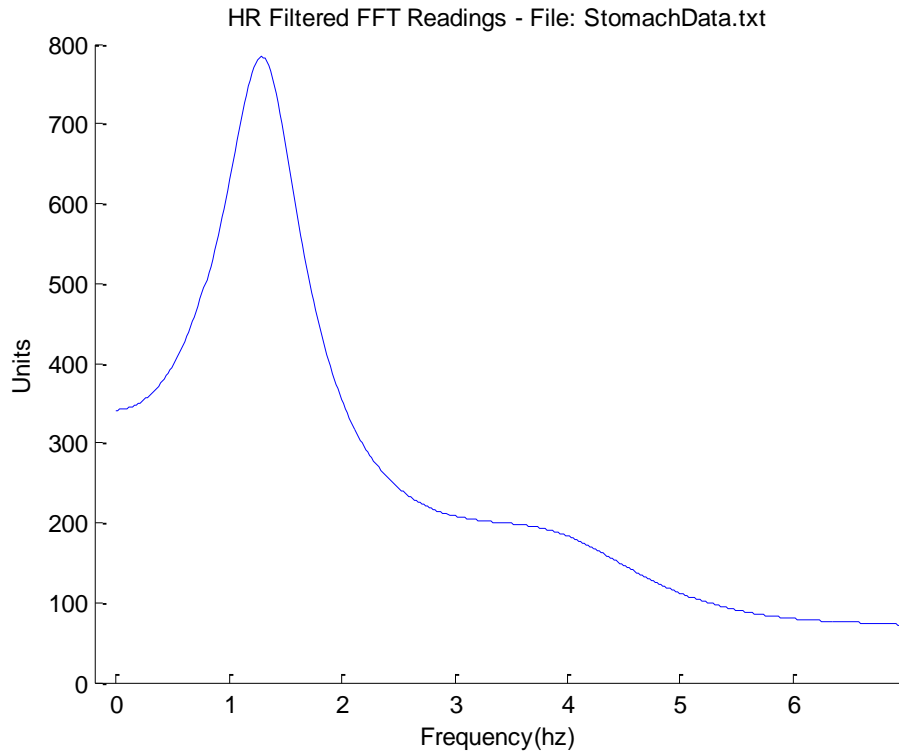


**Figure 8. Magnitude spectrum obtained using linear predictive coding.**

After noting improvements of each time-domain manipulation, the conclusion was reached that LPC provides a more distinct heart rate in the frequency domain if LPC is conducted *after* the autocorrelation rather than when LPC is used alone. Using LPC after an autocorrelation makes the heart rate more distinct and adds a smoothing feature to lower the noise around the peak, or heart rate. Figure 9 contains a magnitude spectrum that results from autocorrelation followed by LPC. The spectrum displays a distinct peak when compared to the spectrum obtained from the LPC-only results illustrated in Figure 8. A significant narrowing of the peak occurred, which provides greater accuracy over any of the spectra displayed in the previous figures.

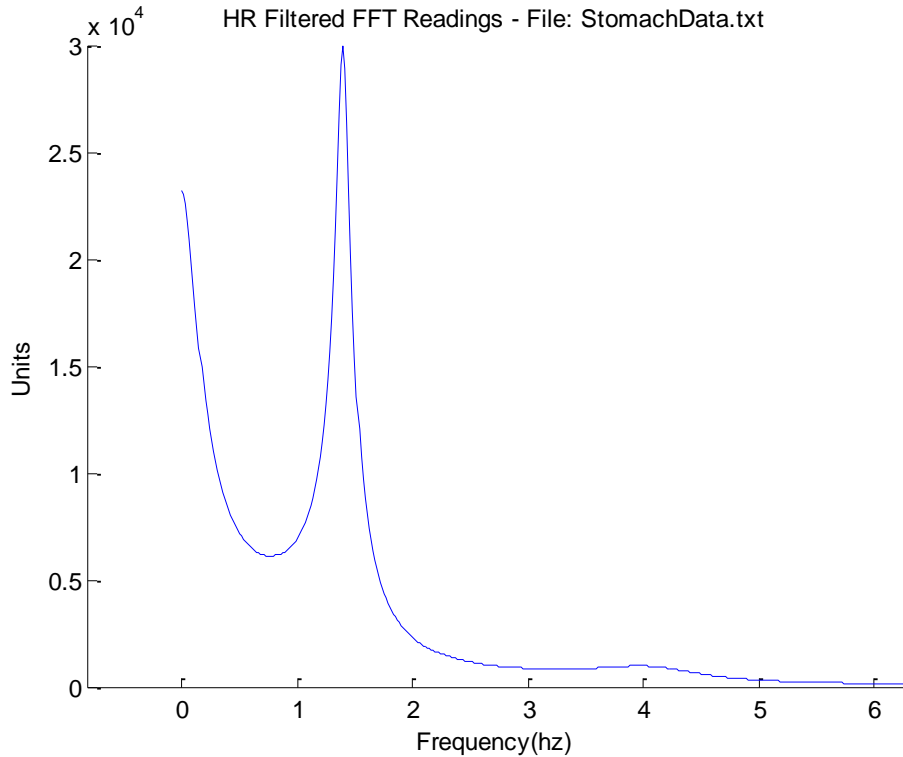


**Figure 9. Magnitude spectrum obtained using both autocorrelation and LPC.**

### ***3.4.4 Heart Rate Estimation***

Previous work with autocorrelation and LPC has resulted in means to increase the accuracy of heart rate determination in the frequency domain. Almost all electrocardiographs (ECGs) and pulse oximeters, the most common devices used to measure heart rate, display a heart rate reading every few seconds and utilize an internal averaging algorithm, since heart rates fluctuate from beat to beat in normal individuals. Therefore, the algorithms described in the previous sections can be implemented in MathScript and applied to every 10 seconds of data to obtain accurate results while maintaining a consistent reporting time frame. Since LPC minimizes the least squares error, one can determine the frequency of the maximum peak for a given interval and use this as the heart rate over the entire span of the interval. For this study, 37 Hz and 121 Hz were used as the max and min heart rate values (upper and lower heart rate bounds), which are dynamic with sample rate.

Once the time frame and upper and lower bounds are set, several peaks can occur in the frequency domain between these upper and lower bounds. Figure 10 illustrates an ideal magnitude spectrum for someone with a heart rate of approximately 60 bpm. The first peak is

higher than the second peak at the desired heart rate, and the second peak, whether from harmonics or vascular reflections, is over 0.5 Hz away from the correct peak so that the algorithm does not identify it as a false positive.

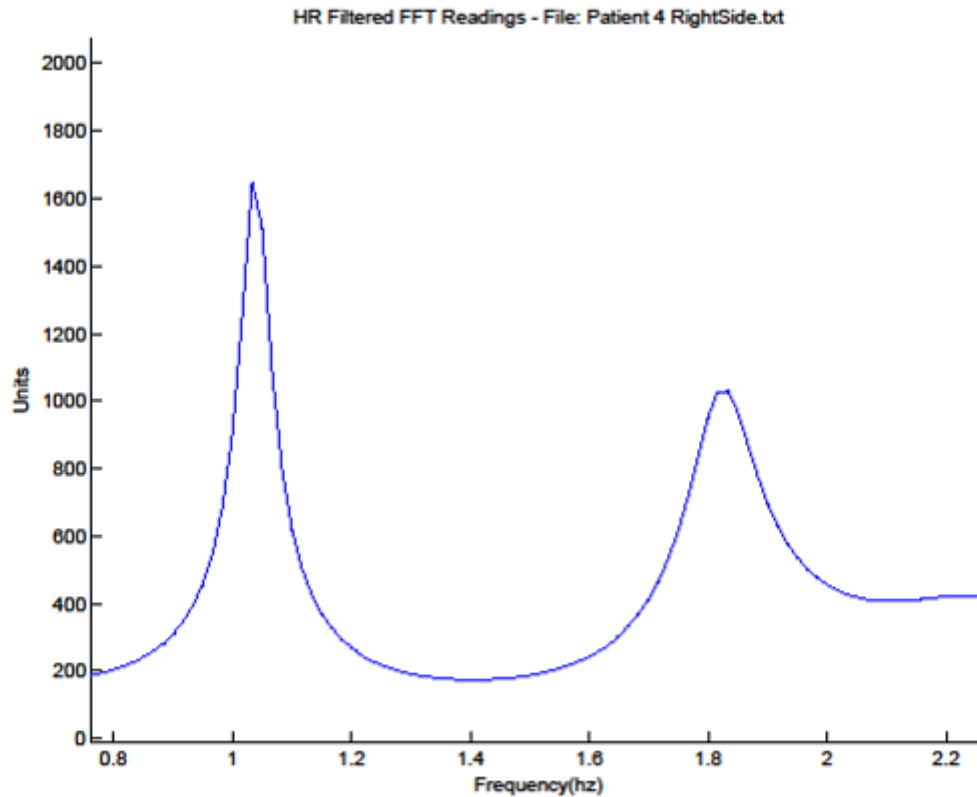


**Figure 10. Ideal magnitude spectrum for determining heart rate.**

Figure 11 illustrates a non-ideal magnitude spectrum with a peak around 120 Hz which is larger than the peak around 60 bpm even though the peak at 60 bpm is at the true heart rate (i.e., as determined by a commercial pulse oximeter). A third peak in the middle of the first and last peak could also trick the algorithm into identifying a false positive.

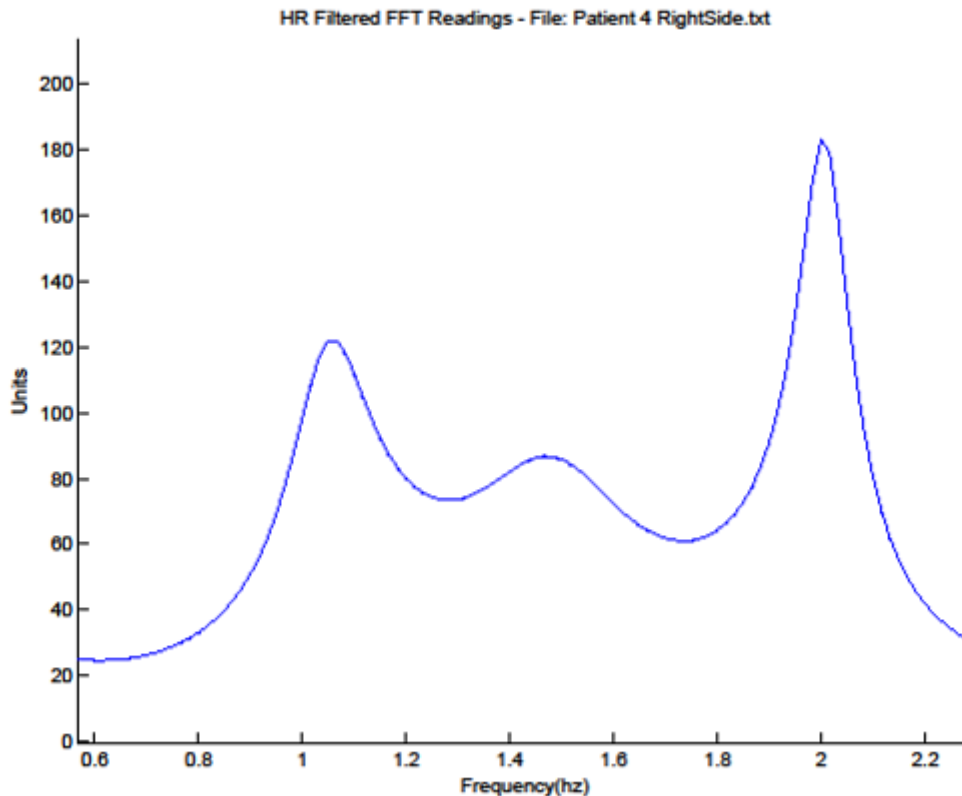


**Figure 11. Non-ideal magnitude spectrum for determining heart rate.**

For this study, an algorithm was designed to find the most accurate peak to use as the heart rate estimation given the subject data available from the members of the research team. The algorithm used a method that kept a weighted guess of what the heart rate could be and used the closest peak to that number. This weighted guess was an algorithm that averaged several peaks found, including previous heart rate estimates, the current heart rate estimate, the closest peak to a target frequency, and the highest maximum peak. The estimate was averaged with the previous three heart rate estimates to offer a specific frequency to identify at the next heart rate peak. This heart rate detection algorithm was designed to identify any heart rate; the previous heart rate and current heart rate were used to weight the algorithm in order to closely investigate previous values since many people's resting heart rates remain relatively stable. The target frequency ensured that the algorithm was constrained to the area near the average heart rate in case the algorithm began to choose incorrect peaks consistently in the heart rate frequency, such as an alternate harmonic. Finally, the highest peak was closest to the heart rate that a commercial pulse oximeter displayed a majority of the time peaks were analyzed, so the maximum peak was taken



into account to prevent the algorithm from accidentally acquiring a peak that was further away from the reading that the pulse oximeter showed consistently. The target frequency used was 60 bpm, which is sensible for many people in a resting state, but the target frequency could be greatly improved if the person's average heart rate was known and inserted for the target frequency. After completing the heart rate estimation, a five-wide sliding median filter was performed across the data to remove outliers.

### **3.5 Process for Participants**

For this study, the circuit was placed on a lab bench and powered by a Sorensen XPH-35-4T power supply. The electromechanical film was placed in the middle of the bed where a participant's chest should be, and the film was attached to the circuit through a ribbon cable. The output of the circuit and ground were attached to the Ai0+ and Ai0- channels of a myDAQ unit, which was connected to a computer through a USB interface. Each subject began the experiment by lying on their stomach with the electromechanical film directly under them, a pulse oximeter probe attached to their finger, and a pillow under their head. A technician operated the computer and kept track of the three-minute time period during which data were taken. Another technician recorded heart rate data approximately every 4 seconds. At three-minute intervals, the participant would move to his/her right side, left side, and then back; each time a data set was gathered, the electromechanical film remained directly under the participants, and heart rate values from the pulse oximeter were recorded.

## Chapter 4 - Results

This chapter provides results obtained from operating the data acquisition system and running the heart rate detection algorithm discussed in this report. MathScript was run through LabVIEW to gather data, and then MATLAB was used to rerun the algorithm over the data. Results include heart rate estimation every 10 seconds throughout each of the 16 three-minute-long data sets. The data sets were acquired from four participants lying in four positions on a bed (right side, left side, stomach, and back) with an electromechanical film under them that gathered BCG data for each three-minute interval. Results were then compared to values obtained from a commercial BCI 3180 pulse oximeter whose finger probe was attached to the subject during each gathered data set.

### 4.1 Measurements

Figures 12 through 27 depict the heart rate values obtained from the 16 sets of BCG data acquired from the four subjects. In each case, heart rate values displayed by the BCI pulse oximeter are represented with black circles, whereas heart rate estimates based on BCG data are represented with gray boxes. The figures are ordered by subject number: Subject 1's complete data first (back, stomach, right side, and left side), followed by Subject 2's data, etc. The algorithm presented in Chapter 3 was often the least accurate on the first 10-second heart rate estimate (the first gray box in a given figure), because several peaks would occur in the frequency domain (as illustrated in Figure 11) and the algorithm would be unable to discern which peak to use based on prior heart rate values. Therefore, several starting values had a higher error, consequently causing the next few 10-second heart rate estimates to have higher errors than desired (e.g., as demonstrated in Figures 12 and 24). When the algorithm was less accurate than desired in other instances, a subject's heart rate had increased or decreased quickly, and the algorithm estimated the heart rate as the second of three peaks (the situation illustrated in Figure 9). Examples of this situation are noted in Figures 13 and 25, where the middle portion of the graph is about 10 to 15 bpm higher than it should be, or in Figure 22, where the graph is about 10 to 15 bpm lower than it should be.

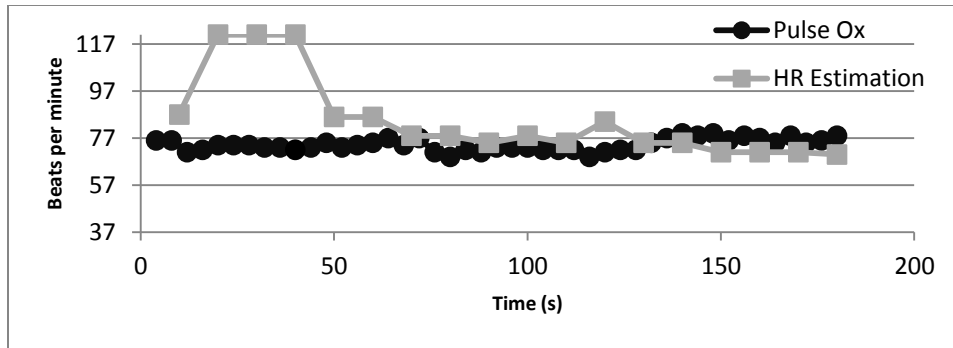


**Figure 12. Heart rate data from Subject 1 lying on their back.**

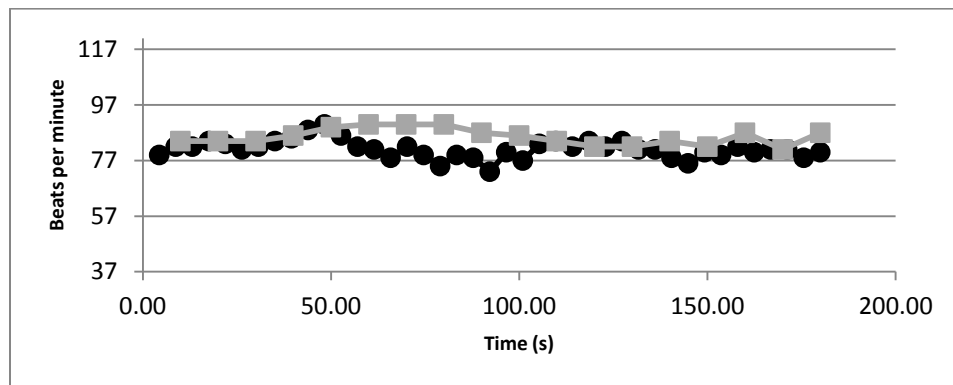


**Figure 13. Heart rate data from Subject 1 lying on their stomach.**

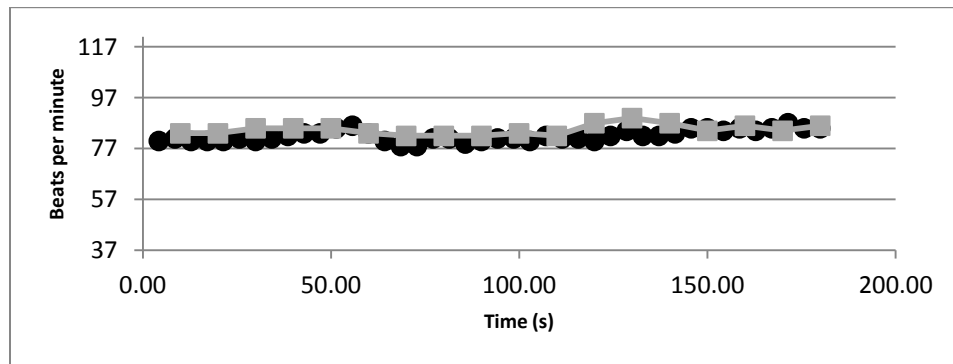


**Figure 14. Heart rate data from Subject 1 lying on their right side.**

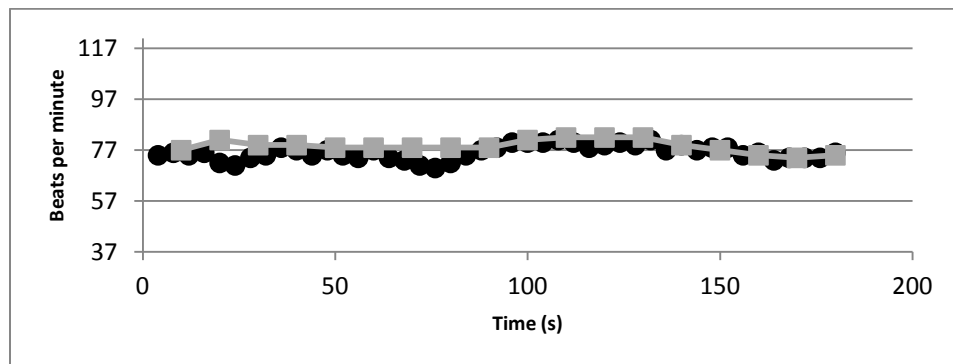


**Figure 15. Heart rate data from Subject 1 lying on their left side**

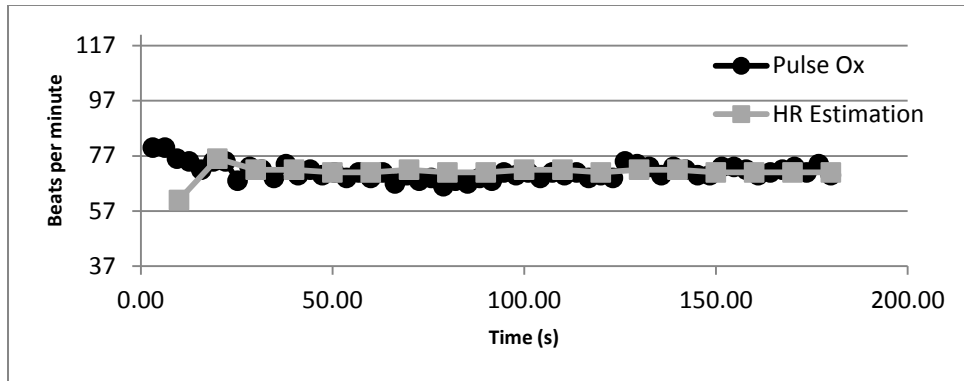


**Figure 16. Heart rate data from Subject 2 lying on their back**

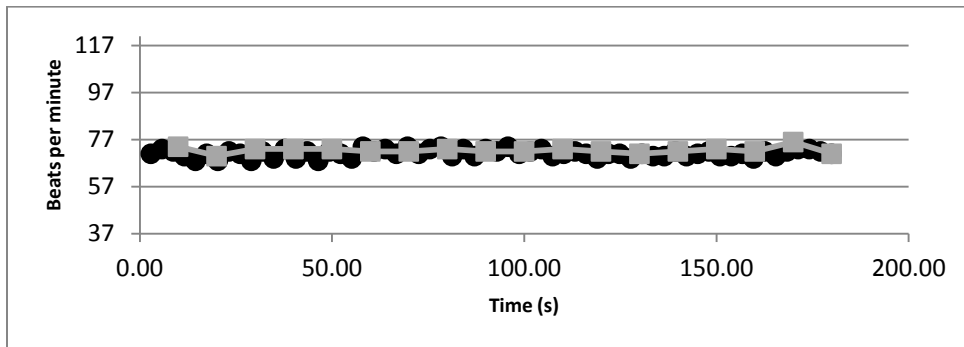


**Figure 17. Heart rate data from Subject 2 lying on their stomach.**

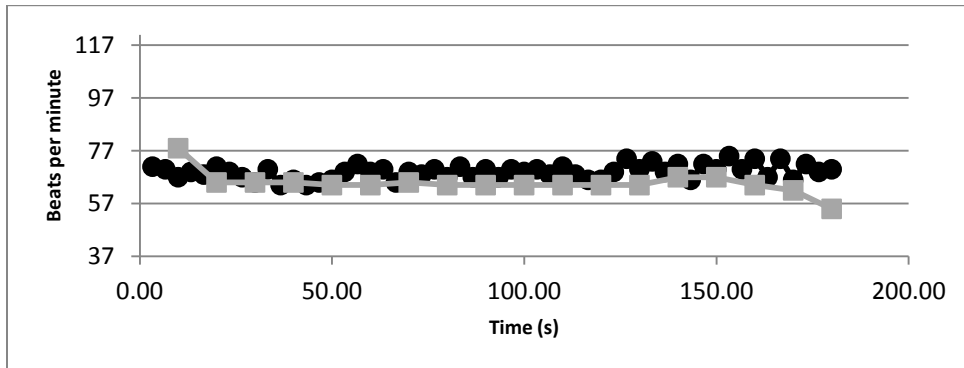


**Figure 18. Heart rate data from Subject 2 lying on their right side.**

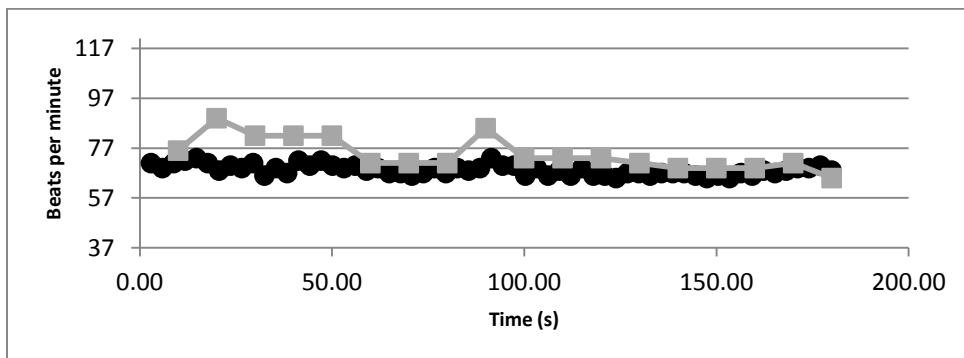


**Figure 19. Heart rate data from Subject 2 lying on their left side.**

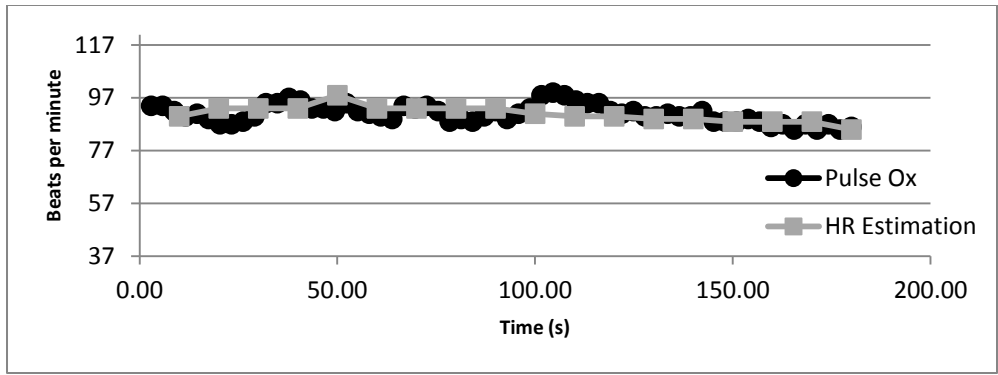


**Figure 20. Heart rate data from Subject 3 lying on their back.**

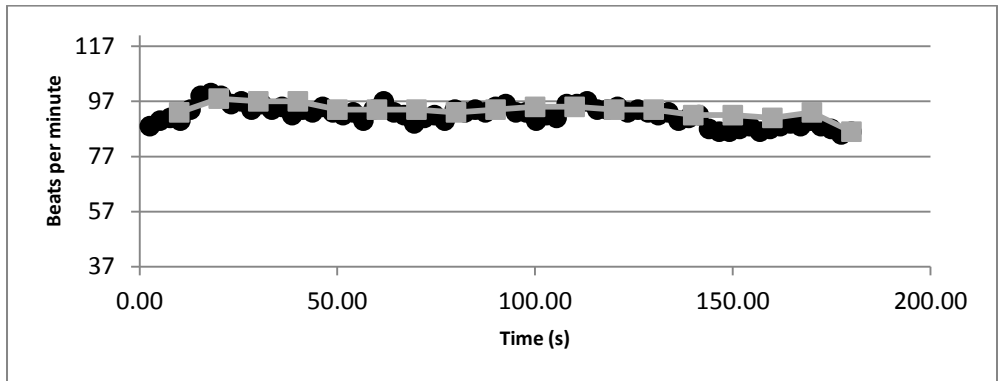


**Figure 21. Heart rate data from Subject 3 lying on their stomach.**

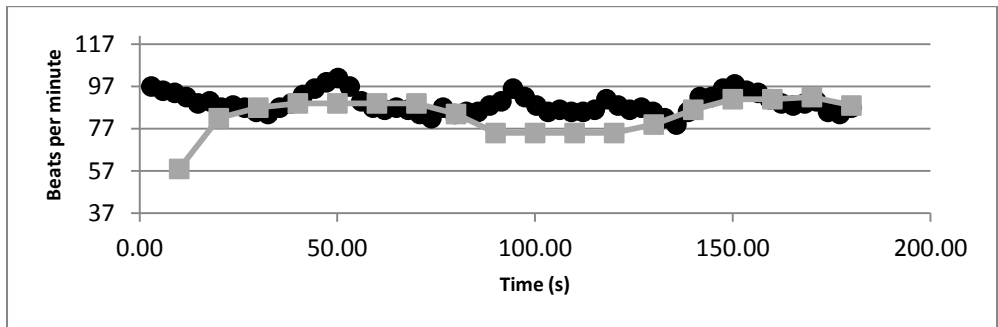


**Figure 22. Heart rate data from Subject 3 lying on their right side.**

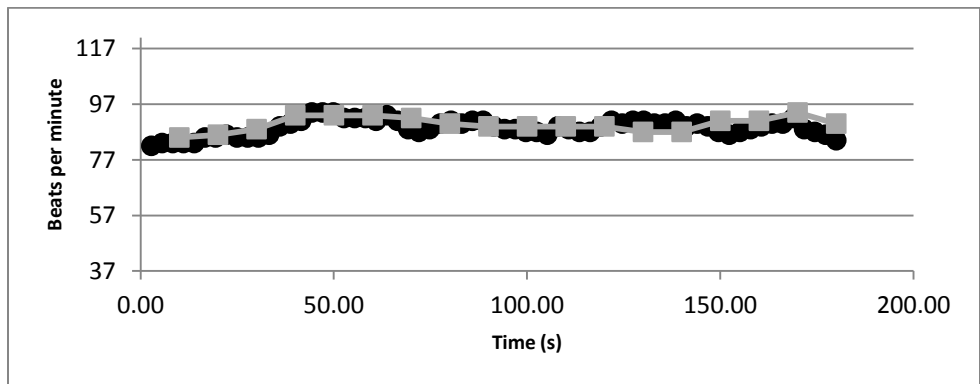


**Figure 23. Heart rate data from Subject 3 lying on their left side.**

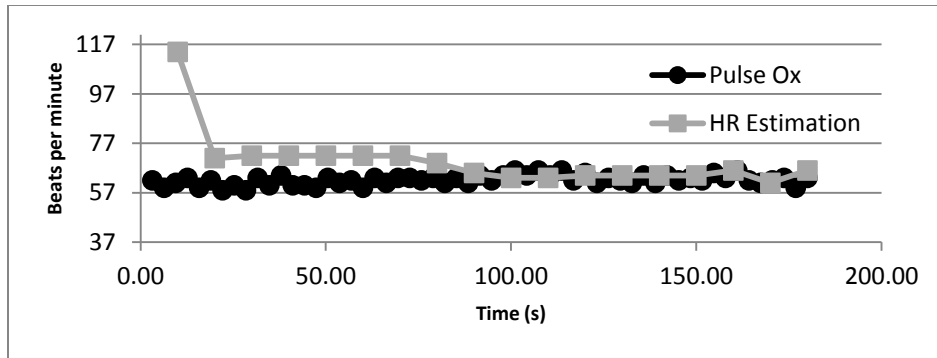


**Figure 24. Heart rate data from Subject 4 lying on their back.**

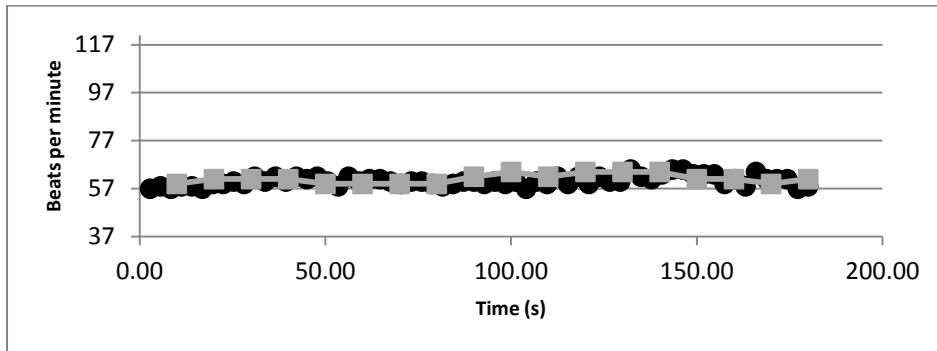


**Figure 25. Heart rate data from Subject 4 lying on their stomach.**

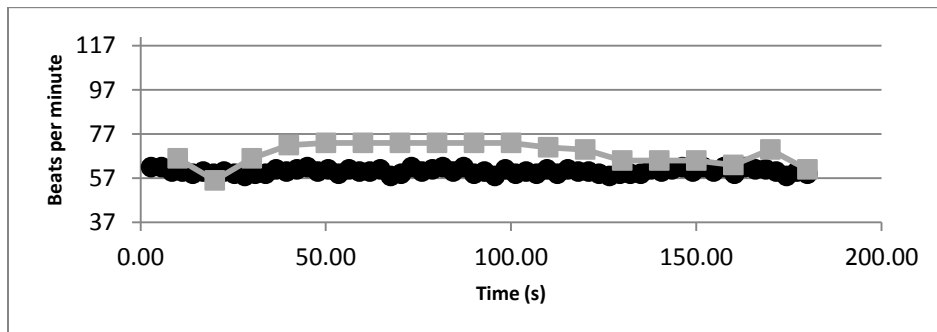


**Figure 26. Heart rate data from Subject 4 lying on their right side.**

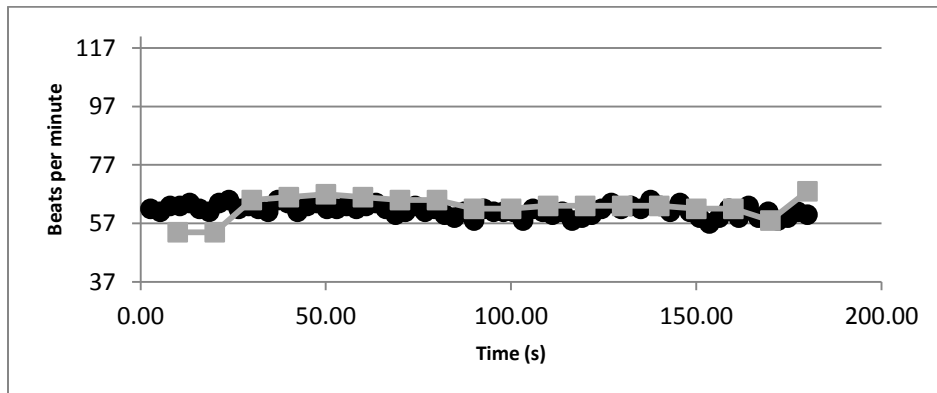


**Figure 27. Heart rate data from Subject 4 lying on their left side.**

## 4.2 Subject Results

Calculated heart rates were compared to the corresponding values displayed on the commercial pulse oximeter, and then these errors were evaluated to determine the average error, the standard deviation of the error, and the overall error. These values are tabulated in Table 1. More specifically, the first error percentage (Table 1, column 2) resulted from comparing each 10-second heart rate estimate in each data set to the corresponding value observed on the pulse oximeter. The magnitudes of these errors were then averaged for all 16 samples. The standard deviation of those errors is noted in Table 1, column 3. The overall error percentage (Table 1, column 4) resulted from comparing the average heart rate estimate over the entire three-minute interval to the average heart rate displayed by the pulse oximeter. Standard deviations of the 16 heart rate estimates for each data set are shown in Table 1, column 5.

**Table 1. Error and standard deviation for all data sets.**

Data Set	Error Avg	Error St Dev	Overall Error
Subject 1 Back	8.8%	5.03	4.7%
Subject 1 Stomach	5.6%	4.56	5.4%
Subject 1 Right Side	3.3%	2.19	2.8%
Subject 1 Left Side	3.5%	2.95	3.1%
Subject 2 Back	2.9%	4.97	0.2%
Subject 2 Stomach	2.2%	1.69	1.8%
Subject 2 Right Side	7.5%	4.67	6.2%
Subject 2 Left Side	9.7%	7.12	9.2%
Subject 3 Back	2.7%	1.96	0.0%
Subject 3 Stomach	2.0%	1.55	1.7%
Subject 3 Right Side	8.4%	9.04	6.7%
Subject 3 Left Side	2.8%	1.64	1.5%
Subject 4 Back	13.2%	19.45	12.1%
Subject 4 Stomach	3.5%	1.94	1.4%
Subject 4 Right Side	14.1%	6.78	13.5%
Subject 4 Left Side	5.4%	4.10	1.9%

An expected higher-percentage error occurred on a point-by-point basis: when each 10-second segment was compared and averaged. While the total error for each three-minute period determined if the data set was an accurate approximation over the whole three-minute period, a more accurate assessment of how closely the algorithm follows the heart rate in 10-second time windows was achieved when the single 10-second errors were averaged. With total data set

errors as low as 0% or 0.2% (e.g., for Subjects 2 and 3 lying on their backs), the electromechanical film method works well for certain three-minute intervals. The other error (the 10-second errors averaged, as in Table 1, column 2), only went as low as 2.0%, but for most subjects, a 2% error would only be one or two bpm. Some data sets had errors as large as 14.1%, which implies poor BCG signal quality possibly resulting from poor body contact with the electromechanical film, non-ideal electromechanical film positioning, or subject movement. These data sets were acquired in the middle of the day while the subjects were awake and other people were present, possibly adding noise to the BCG signal. In addition, most subjects had less accurate results with specific positions: Patient 1 lying on their back, Patient 2 lying on their left side, and Patients 3 and 4 lying on their right side. Although each subject had unique worst data sets, every subject's most accurate data set was provided when they laid on their stomach, according to error percentages.

These results indicate that each subject has positions that accurately allowed for heart rate tracking, with seven of the 16 data sets offering a total error below 2%. However, a position always existed that offered an error several times the error of that subject's best error, and two data sets from an individual had over 10% total error.

Table 2 shows overall statistics averaged for each subject in the various positions from which data were acquired. The stomach position was the most accurate overall, followed by the left side, the back, and the right side. The stomach as an optimal position makes sense, as the heart and lung activity are transferred to the film through relative pliable tissue. Since the heart is slightly oriented toward the left side of the body, one would expect a better signal from the left side when compared to the signal from the right side, as confirmed in Table 2. However, the right side being a worse position than the back side was unexpected. Whether these discrepancies are due to variations in body composition, small sample size, or both is unclear.

**Table 2. Heart rate error for each position.**

Position	Error Avg	Overall Error
Back	6.9%	4.3%
Stomach	3.3%	2.6%
Right Side	8.3%	7.3%
Left Side	5.4%	3.9%



Finally, Table 3 illustrates how the algorithm performs for the individual subjects. Subject 3 had the lowest error, with a 4% average error in all four positions, and Subject 4 had the highest error, with 9.1% average error in all positions. This error differential from Subject 3 to Subject 4 could have been attributed to size or heart rate of the subjects. Subject 3 had the highest average heart rate (e.g. figures 20 through 23) where Subject 4 had the lowest average heart rate (e.g. figures 24 through 27) and Subject 3 had a much higher weight and girth than Subject 4, although not the highest out of all of the subjects.

**Table 3. Heart rate error for each subject.**

Subject	Error Avg	Overall Error
Subject 1	5.3%	4.0%
Subject 2	5.6%	4.4%
Subject 3	4.0%	2.5%
Subject 4	9.1%	7.2%

## Chapter 5 - Future Work and Conclusions

While the method that employs BCGs acquired with electromechanical film indicates that in certain circumstances it can accurately estimate heart rate, several design elements could be improved upon and tested further. Some examples would include testing the subjects with larger gain or filtering in the circuit and using a more sensitive or larger area electromechanical film; this could be achieved by raising the corner frequency on the preamplifier to over 5 Hz to maintain full heart rate magnitude. Additional testing with the current setup and a greater number of subjects would be beneficial to determine if the results found in this experiment can be generalized. In addition, BCGs obtained while subjects are sleeping would be expected to be cleaner signals that offer more accurate heart rate estimates. Improvements in time-domain filtering, for example finding a better solution than using autocorrelation and linear predictive modeling, could increase the reliability of the system.

The investigation of other parameters such as respiration rate, movement, cardiac parameters, seizures while sleeping, etc. would also enhance this research. Mapping heart rate variability and LPC frequency domain peaks could also be beneficial for algorithm improvement. Furthermore, investigation of the effects of different subject body weights and sizes on signal strength and quality could test the broader viability of this method.

## References

- [1] C. Da-Wei, L. You-De, Y. Chung-Ping, C. Jing-Jhong, C. Ying-Huang, C. Chun-Yu, H. Yu-Cheng, S. Fu-Zen, and L. Sheng-Fu. "Design and Implementation of a Modularized Polysomnography System," *IEEE Transactions on Instrumentation and Measurement*, vol. 61, no. 7, 2012, pp. 1933-1944.
- [2] F. Cortesi, F. Giannotti, A. Ivanenko, and K. Johnson. "Sleep in children with autistic spectrum disorder," *Sleep Med*, vol. 11, no. 7, Aug, 2010, pp. 659-64.
- [3] K. C. Dominick, N. O. Davis, J. Lainhart, H. Tager-Flusberg, and S. Folstein. "Atypical behaviors in children with autism and children with a history of language impairment," *Res Dev Disabil*, vol. 28, no. 2, March-April 2007, pp. 145-62.
- [4] J. Baio. "Prevalence of Autism Spectrum Disorder Among Children Aged 8 Years — Autism and Developmental Disabilities Monitoring Network, 11 Sites, United States, 2010," *Surveillance Summaries*, N. C. o. B. D. a. D. Disabilities, Ed. [www.cdc.gov](http://www.cdc.gov): Centers for Disease Control and Prevention, 2014.
- [5] S. Jianwei, Z. Xuezhou, Z. Xiaodong, T. Jintian, and L. Lei. "Ballistocardiogram Measurement System Using Three Load-Cell Sensors Platform in Chair," 2<sup>nd</sup> *International Conference on Biomedical Engineering and Informatics*, BMEI '09., 17-19 Oct. 2009.
- [6] C. Gih Sung, C. Byoung Hoon, J. Do-Un, and P. Kwang-Suk. "Noninvasive Heart Rate Variability Analysis Using Loadcell-Installed Bed During Sleep," 29<sup>th</sup> *Annual International Conference of the IEEE Engineering in Medicine and Biology Society*, EMBS 2007, 22-26 Aug. 2007.
- [7] E. Ltd. "L-Series sensors specifications." [http://www.emfit.com/uploads/pdf/Emfit\\_L-series\\_specifications.pdf](http://www.emfit.com/uploads/pdf/Emfit_L-series_specifications.pdf), 2003, pp. 1-2.
- [8] O. Postolache, P. S. Girao, G. Postolache, and M. Pereira. "Vital Signs Monitoring System Based on EMFi Sensors and Wavelet Analysis," *IEEE Instrumentation and Measurement Technology Conference Proceedings*, IMTC 2007. IEEE, 1-3 May 2007.
- [9] B. Y. Su, K. C. Ho, M. Skubic, and L. Rosales. "Pulse rate estimation using hydraulic bed sensor," 2012 *Annual International Conference of the IEEE Engineering in Medicine and Biology Society*, Aug. 28 - Sept. 1, 2012.
- [10] Z. Yongwei, Z. Haihong, M. Jayachandran, A. K. Ng, J. Biswas, and C. Zhihao. "Ballistocardiography with fiber optic sensor in headrest position: A feasibility study and a new processing algorithm," 35<sup>th</sup> *Annual International Conference of the IEEE Engineering in Medicine and Biology Society*, 3-7 July 2013.
- [11] E. Ltd. "Preamplifiers for emfit sensors." [http://www.emfit.com/uploads/pdf/Emfit\\_preamplifiers\\_for\\_emfit\\_sensors.pdf](http://www.emfit.com/uploads/pdf/Emfit_preamplifiers_for_emfit_sensors.pdf), 2003, pp. 1-2.
- [12] W. Xu, J. Fangfang, Y. Dan, and L. Yuan. "Estimation of the respiratory component from ballistocardiography signal using adaptive interference cancellation," *Control and Decision Conference (CCDC)*, 2011 (Chinese), 23-25 May 2011.
- [13] E. Ltd. "Calculating the output voltage of emfit sensors." [http://www.emfit.com/uploads/pdf/Emfit\\_Calculating\\_the\\_output\\_voltage\\_of\\_emfit\\_sensors.pdf](http://www.emfit.com/uploads/pdf/Emfit_Calculating_the_output_voltage_of_emfit_sensors.pdf), 2003, pp. 1.
- [14] A. Devices. "Ultralow Distortion, Ultralow Noise Op Amp AD797." [http://www.analog.com/static/imported-files/data\\_sheets/AD797.pdf](http://www.analog.com/static/imported-files/data_sheets/AD797.pdf).

- [15] M. Dendrinis and G. Carayannis. "Spectrum analysis using a new autocorrelation measure," *1988 International Conference on Acoustics, Speech, and Signal Processing, ICASSP-88*, 11-14 April 1988.
- [16] A. Harma and U. K. Laine. "A comparison of warped and conventional linear predictive coding," *IEEE Transactions on Speech and Audio Processing*, vol. 9, no. 5, 2001, pp. 579-588.

## Appendix A - MATLAB Script

```
%Script Name: graphBCG
%Author: Steve Rubenthaler
%Data: 8/12/2014
%Input Parameters: filename is the name of the file with the data set.
%sr is the sample rate that the data set was taken at.
%Output Parameters: HR is used to keep track and return values when
%graphBCG is used
%HR(1) = max value in data set, HR(2) = closest peak to 60bpm
%HR(3) = closest peak to HRAvg2, HR(4) = averaged heart rate estimation
%HR(5) = max peak in bounds, HR(6) = how many peaks in bounds
%HR(7) = final heart rate estimate
%this script takes a data set of raw BCG data, filters it and gives a
heart rate estimation for each ten second interval.
function [HR] = graphBCG (filename,sr) % file name and sample rate
if ischar(filename);
    amplitudel = load(filename); %load all amplitude readings
else
    amplitudel = filename;
end

HRPrev = [1 1 1]; % set up Previous heart rate array
HRAvg2 = 1; % set the heart rate average to 60bpm

for i = 1:length(amplitudel)/(sr*10), % loops though the whole data set
in increments of 10 seconds
    amplitude = amplitudel(((i-1)*150*10)+1:(i)*150*10,1); % gets 10
seconds of data
    dt = 1/sr;
    time = 0:dt:(length(amplitude)-1)*(dt); % set time for all readings

%sets the high and low of amplitude
high = max(amplitude);
low = min(amplitude);

[lengthAmp,g] = size(amplitude); % gets the size of amplitude
```

```

%sets the corner and stop frequencies
Fc = .75;
Fst = 1.5;

%sets the filter width of the high pass filter to be dynamic with
sample rate
%then does the filter and trims off the unreliable numbers
filter1width = 2*round((sr/Fc)/2);
c = firls(filter1width,[0 Fc/(sr/2) Fst/(sr/2) 1],[0 0 1 1]);
filter1 = filter(c,1,amplitude);
filter1trim = filter1((filter1width):lengthAmp,1);

%sets the filter width of the low pass filter and stop frequency
%does a low pass filter and then trims off the unreliable numbers
filter2width = 3;
stopfreq = 2;
[b, a] = butter(filter2width, stopfreq./(sr/2), 'low');
filter2 = filter(b,a,filter1trim);

%sets HeartRate to the filtered data minus any unreliable numbers
[lengthFilter2,g] = size(filter2);
HeartRate = filter2(filter2width:lengthFilter2,1);

%sets the max and min for HeartRate and gets the time interval
highHR = max(HeartRate);
lowHR = min(HeartRate);
timeHR = 0:dt:(length(HeartRate)-1)*(dt);

%performs an FFT of the data that has been filtered with high and low
pass filters
NFFT = 2^nextpow2(lengthAmp); % Next power of 2
Y = fft(amplitude,NFFT)/lengthAmp;
Yabs = 2*abs(Y(1:NFFT/2+1));
f = sr/2*linspace(0,1,NFFT/2+1);
highfft = max(Yabs);
lowfft = min(Yabs);

%performs an autocorrelation on the filtered signal

```

```

FiltYabsHR=xcorr(HeartRate,'coeff');
[lengthFiltYabsHR,g] = size(FiltYabsHR);
FiltYabsHRmid =
FiltYabsHR(round(lengthFiltYabsHR*.25):round(lengthFiltYabsHR*.75),1);
[lengthFiltYabsHRmid,g] = size(FiltYabsHRmid);

%performs an FFT on the autocorrelated signal
%then makes a time variable and finds the max and min values for
graphing
FiltNFFTTHR = 2^nextpow2(lengthFiltYabsHRmid); % Next power of 2
FiltYHR = fft(FiltYabsHRmid,FiltNFFTTHR)/lengthFiltYabsHRmid;
FiltYabsHRFFT = 2*abs(FiltYHR(1:FiltNFFTTHR/2+1));
fHR = sr/2*linspace(0,1,FiltNFFTTHR/2+1);
highfiltHR = max(FiltYabsHRmid);
lowfiltHR = min(FiltYabsHRmid);

%performs linear predictive coding and transfers it to a freq domain
P = 256;
HRLPC = lpc(FiltYabsHRmid,P);
HRres = (sr/2)/(1/60);
[HRLpc, radLPC] = freqz(1,HRLPC,HRres);
timeLPC=radLPC*(sr/(2*pi));

%graphs the final freq domain of the fully filtered data
figure;
hold on;
plot(timeLPC,abs(HRLpc));
title(sprintf('HR Filtered FFT Readings - File: %s', filename));
xlabel('Frequency(hz)');
ylabel('Units');
hold off;

%sets the upper and lower bounds of heart rate at 37Hz and 121Hz
HRlower = round(.6/((sr/2)/HRres));
HRupper = round(2/((sr/2)/HRres));

%finds the max value inbtween the upper and lower bounds
[C,H_R] = max(abs(HRLpc(HRlower:HRupper,1)), [], 1);

```

```

%Records the max value
HR(i,1) = ((H_R+HRlower)*((sr/2)/HRres))*60;

%finds all peaks in the final freq domain of the signal and scales them
[pks,locs] = findpeaks(abs(HRlpc));
locs=locs*(1/60);

%finds the closes peak to 60bpm and records it in HR
%uses upper or lower bounds if it cannot find one
HRAvg1 = 1;
i_lower1 = find(locs <= HRAvg1,1,'last');
i_higher1 = find(locs >= HRAvg1,1,'first');
lower_than_HRAvg1 = locs(i_lower1);
higher_than_HRAvg1 = locs(i_higher1);
if abs((lower_than_HRAvg1 - HRAvg1)) < abs((higher_than_HRAvg1 -
HRAvg1))
    if lower_than_HRAvg1 > .616
        HR(i,2) = lower_than_HRAvg1*60;
    else
        HR(i,2) = 37;
    end
else
    if higher_than_HRAvg1 < 2
        HR(i,2) = higher_than_HRAvg1*60;
    else
        HR(i,2) = 121;
    end
end

%finds the largest peak in-between the upper and lower limits of heart
rate
if(1)
    validlocs = find(.616 < locs & locs < 2);
    Maxpks = 0;
    MaxpksLoc = 0;
    for j = 1:length(validlocs),
        HR(i,6) = length(validlocs);
        if(pks(validlocs(j))>Maxpks)

```



```

        Maxpks = pks(validlocs(j));
        MaxpksLoc = locs(validlocs(j));
    end
end
if MaxpksLoc ~= 0
    HR(i,5) = MaxpksLoc*60;
end
end

%changes the HRAvg2 based off of the largest peak and the peak found
closest to 60bpm
%also sets the HRRrev first value to the same thing
%this is done only the 1st iteration to try and predict the 1st heart
beat more accurately
if(i==1)
    HRAvg2 = (HR(i,2)+HR(i,5))/120;
    HRPrev(1,1) = (HR(i,2)+HR(i,5))/120;
end

%finds the closes peak to HRAvg2 and records it in HR
%uses upper or lower bounds if it cannot find one
i_lower2 = find(locs <= HRAvg2,1,'last');
i_higher2 = find(locs >= HRAvg2,1,'first');
lower_than_HRAvg2 = locs(i_lower2);
higher_than_HRAvg2 = locs(i_higher2);
if abs((lower_than_HRAvg2 - HRAvg2)) < abs((higher_than_HRAvg2 -
HRAvg2))
    if lower_than_HRAvg2 > .616
        HR(i,3) = lower_than_HRAvg2*60;
    else
        HR(i,3) = 37;
    end
else
    if higher_than_HRAvg2 < 2
        HR(i,3) = higher_than_HRAvg2*60;
    else
        HR(i,3) = 121;
    end
end

```

```

end

%sets HR(4) (the final estimate) depending on the values of the other
peaks
%HR is used to keep track and return values when graphBCG is used
%HR(1) = max value in data set, HR(2) = closest peak to 60bpm
%HR(3) = closest peak to HRAvg2, HR(4) = averaged heart rate estimation
%HR(5) = max peak in bounds, HR(6) = how many peaks in bounds
%HR(7) = final heart rate estimate
if(HR(i,2)==121||HR(i,2)==37)
    HR(i,4)= HR(i,3);
else
    if(HR(i,3)==121||HR(i,3)==37)
        HR(i,4)= HR(i,3);
    else
        if(i==1)
            HR(i,4) = (HR(i,2)+HR(i,5)+HR(i,5))/3;
        else
            HR(i,4) = (HR(i-1,3)+HR(i,3)+HR(i,2)+HR(i,5))/4;
        end
    end
end
end

%sets the HR(7) the final heart rate estimate
if(HR(i,2)==HR(i,5))
    HR(i,7) = HR(i,2);
else if(HR(i,3) == HR(i,5))
    HR(i,7) = HR(i,3);
else
    HR(i,7) = HR(i,3);
end
end

%keeps track of the previous 3 average heart rate estimates
%these are averaged to give the next HRAvg2 heart rate target
HRPrev = circshift(HRPrev,[0 1]);
if(HR(i,4)==37 || HR(i,4) ==121)
    HRPrev(1,1) = 1;

```

```
else
    HRPrev(1,1) = (HR(i,4))/60;
end
HRAvg2 = mean(HRPrev);

end

end
```